A DISCRETE BOND MODEL FOR 3D ANALYSIS OF TEXTILE REINFORCED AND PRESTRESSED CONCRETE ELEMENTS

DISKRETES VERBUNDMODELL FÜR 3D-FE-BERECHNUNGEN VON TEXTILBEWEHRTEN UND VORGESPANNTEN BETONKONSTRUKTIONEN

UN MODELE DISCRET DE L'ADHERENCE POUR L'ANALYSE 3D DE STRUCTURES EN BETON RENFORCEES ET PRECONTRAINTES AVEC DES ARMATURES TEXTILES

Markus Krüger, Joško Ožbolt, Hans-W. Reinhardt

SUMMARY

Textile reinforced concrete structures show several significant advantages compared to steel reinforced concrete structures which are well known up to now. However some disadvantages like the low utilization factor of the textile reinforced elements become obvious. As in any reinforced structure, a transfer of forces from reinforcement to concrete is accomplished through bond. Therefore understanding and further improvement of bond properties between textile and concrete is important. In the paper bond properties between different textiles and high performance fine grain concrete are discussed.

Numerical simulations with a variation of input data were performed using a nonlinear finite element code based on the microplane model for concrete and the discrete bond model. The bond model is based on a discrete Finite elements formulation which can be used for steel reinforced concrete as well. The numerical simulations and variation of parameters show the influence of different bond characteristics of textile reinforcements and therefore give some hints on possible optimisation of textile structures.

ZUSAMMENFASSUNG

Wie bereits in der neueren Literatur erwähnt, zeigen textile Bewehrungsmaterialien in verschiedenen Anwendungsgebieten deutliche Vorteile gegenüber konventioneller Stahlbewehrung. Aber auch einige Nachteile wie die geringe nutzbare Festigkeit textiler Bewehrung in Betonbauteilen und die damit verbundenen hohen Kosten sprechen gegen einen Einsatz solcher Bewehrungsmateria-

lien. Im Allgemeinen kommt dem Verbund zwischen Bewehrung und Beton bei derartigen Verbundwerkstoffen eine hohe Bedeutung zu, sind diese doch unter anderem maßgebend für das Tragverhalten. Im vorliegenden Beitrag werden daher wesentliche Verbundeigenschaften verschiedener textiler Bewehrungen in Beton diskutiert und erläutert.

Anhand von nichtlinearen Finite-Element-Berechnungen mit Parametervariationen wird ein neues Verbundmodell zur Charakterisierung textiler Bewehrungen in Beton vorgestellt. Das in den FE-Code MASA eingebundene Verbundmodell basiert im Wesentlichen auf den gleichen Annahmen wie sie für den Stahl-/Betonverbund gelten und wurde in einigen wenigen Punkten für textile Bewehrungen angepasst. Numerische Simulationen zeigen, wie Einflüsse textiler Bewehrungen aufgrund unterschiedlicher Struktur und Art berücksichtigt und wie zudem textile Bewehrungen hinsichtlich des Tragverhaltens textilbewehrter Bauteile optimiert werden können.

RESUME

Les armatures textiles ont plusieurs avantages significatifs par rapport aux armatures conventionnelles en acier. Cependant certains inconvénients comme le bas taux d'exploitation de la résistance de l'armature textile et les coûts élevés qui en résultent s'opposent à leur application à grande échelle. L'adhérence entre l'armature et le béton joue un rôle important dans les matériaux composites, elle est souvent décisive pour le comportement sous charge d'une structure. Dans l'article présent, les caractéristiques de l'adhérence de différentes armatures textiles sont décrites et discutées.

Des simulations numériques avec une variation des paramètres ont été effectués en utilisant des éléments finis non-linéaires basés sur le modèle "microplane" pour le béton et le nouveau modèle discret de l'adhérence. Le modèle de l'adhérence est basé sur un modèle discret de l'adhérence qui peut être également employé pour le béton avec une armature en acier. Les simulations numériques et la variation des paramètres montrent l'influence de différentes caractéristiques de l'armature textile. On peut en déduire des mesures pour optimiser le comportement des structures avec des armatures textiles.

KEYWORDS: uncoated textiles, impregnated textiles, concrete, Carbon, AR glass, bond, bond model, 3D FE analysis, prestress

INTRODUCTION

Bond behaviour of textile reinforcement in concrete is expected to vary from that of FRP bars or conventional steels bars. Most textile rovings used as concrete reinforcement consist of thousands of single filaments and therefore can not be defined as a single rod. If such a roving is embedded in concrete the shape of the cross section determines the bonded area and it must be clarified how many filaments were in direct contact with concrete. A great deal of research has been done recently to characterize bond behaviour of such multifilament elements in concrete but quite new innovations necessitate further research /BRAMESHUBER, 2000/, /NAMMUR, 1989/, /OHNO, 1994/. Moreover quite a number of experimental investigations have been carried out to understand bond behaviour of prestressed and/or impregnated textiles or rovings.

One parameter that may strongly influence the bond performance is the difference in the coefficient of thermal expansion from that of steel or concrete. It is also known that transverse pressure improves bond which is neglected in many bond models. However, this effect seems to be not important for embedded multi-filament rovings which have not been fully infiltrated with cement due to voids between the inner filaments. Despite this the Poisson's effect becomes significant and influences the transverse stress field if the roving is impregnated and/or prestressed. Some test results of carbon reinforced and prestressed specimen are illustrated in Figure 1 /KRÜGER, 2001B/.

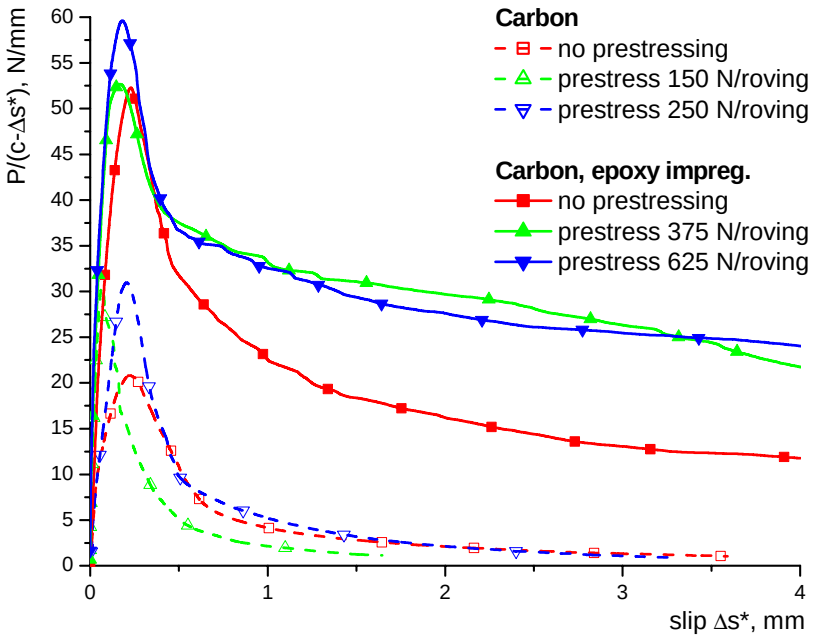

Figure 1: Bond stress per unit length versus slip based on 20mm double sided pull-out (stored at 20°C, 65% RH for 40 days) /KRÜGER, 2001B/

It can be seen that an impregnation of a carbon roving with an epoxy resin generally results in a better bond whereas a roving that was not impregnated shows a low maximum bond stress and after bond failure a very low frictional resistance. It is assumed that the main reason for this is the ribbed surface formed by the binder threads and the change of the roving diameter over its length, especially at the crossing points where the perpendicular woof roving is fixed. The binder threads are caused by the warp knitting process (Figure 2) and were fixed by the epoxy resin. It can be seen from figure 1 that prestressing leads to a higher bond strength. As discussed above, bond performance of textile reinforcement in concrete depends on many different parameters. This leads us to consider a formulation of a such bond model in which these aspects would be accounted for.

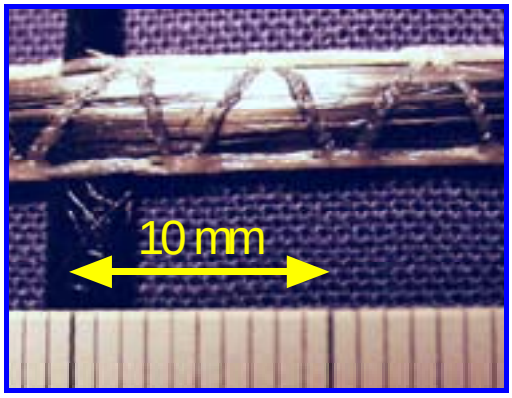

Figure 2: Detail of an epoxy impregnated carbon fabric

DISCRETE BOND MODEL FOR FINITE ELEMENT ANALYSIS

For numerical studies the bond properties between textiles and concrete, discrete elements were used. The bond model proposed by /OŽBOLT, 2002/ has therefore been modified for textile reinforcement and used together with solid finite elements in a 3D FE studies.

In the numerical studies bond between the textiles and concrete was simulated by discrete bond element that have recently been implemented into 3D FE code MASA /OŽBOLT, 2002/. Concrete, which is discretized by the three dimensional finite elements, is modelled by the microplane model /OŽBOLT, 2001/. The bond elements connect the concrete finite elements with the reinforcement that is represented by the truss finite elements (see Figure 3). Only degrees of freedom in the bar direction are considered. However, beside the tangential stresses parallel to the bar direction, the radial stresses perpendicular to the bar direction are generated as well. It is assumed that at a given slip the radial stress depends on

erated as well. It is assumed that at a given slip the radial stress depends on the geometry of the bar and the bar strain as well as on the geometry and the boundary conditions of the concrete specimen. The interaction between tangential and radial stresses is accounted for in three different ways: (i) directly, the shear stress depends on the nonlocal (representative) radial stress obtained from the concrete elements close to the reinforcing bar, (ii) the local strain of the bar element and its lateral expansion or extension and (iii) indirectly, in a way that the larger shear stress (higher bond strength due to larger ribs or roughness of the bar element) cause higher activation of stresses in the radial direction.

In the present model, splitting of concrete is indirectly accounted for. Namely the interaction between shear and radial stresses results in corresponding tangential tensile stresses that causes cracking of the surrounding non-linear concrete elements and, therefore, failure of bond resistance.

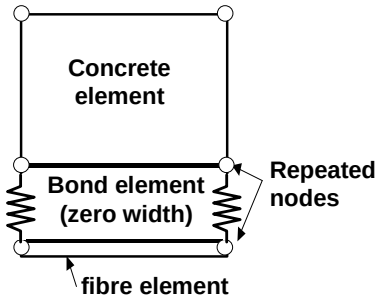

Figure 3: Bond elements with zero width.

Bond stress-slip relation in a 2D consideration

The experimental evidence /CEB BULLETIN 230, 1996/ indicates that the load transfer between reinforcement and concrete is accomplished through bearing of the reinforced steel lugs on surrounding concrete and through friction. As discussed by /YANKELEVSKY, 1987/, the total bond resistance can be decomposed into two components: (i) mechanical interaction component τ_m, and (ii) friction component τ_f. The friction component can be separated into a residual friction τ_r and a virgin friction τ_v component. The residual friction represents frictional resistance upon slip reversal whereas the virgin friction component is due to the additional frictional resistance developed upon loading to previously undeveloped slip levels. It is assumed that textile reinforcement behaves similarly as steel reinforcement does, with the difference that mainly the adhesion of the textile and the roughness of the surface improve the mechanical bond instead of the steel lugs.

Based on the experimental results /ELIGEHAUSEN, 1983/, /MALVAR, 1992/ and as well documented by /LOWES, 2002/, the bond slip relationship of steel reinforcement in concrete can be described by the parameters that are summarized in Table 1. The same parameters are used for textile reinforcement, but in a slightly different manner. The curve of the bond stress versus slip relationship used for the numerical studies is illustrated in Figure 4.

Table1: Summary of the model parameters

Description of the model parameter	Model parameter	
peak mechanical bond strength	$\tau_m = \tau_{m,0}\,\Omega^{*}$	[MPa]
peak frictional bond strength	$\tau_f = \tau_{f,0}\,\Omega^{*}$	[MPa]
peak virgin friction bond strength	$\tau_{f,v} = (1\text{-}0.4)\,\tau_f$	[MPa]
peak residual friction bond strength	$\tau_{f,r} = 0.4\,\tau_f$	[MPa]
secant to bond response curve for initial loading	k_{sec}	[MPa/mm]
slip at which peak bond strength is achieved	$s_1 = (\tau_m+\tau_f)/k_{sec}$	[mm]
slip at which bond strength begins to decrease	$s_2 = s_1+s_2^{*}$	[mm]
slip at which mechanical bond resistance is lost	s_3	[mm]
tangent to the load-displacement curve upon unloading	k_{unload}	[MPa/mm]
initial tangent to the bond-slip response	k_1	[MPa/mm]
tangent to the bond-slip curve at peak resistance	$k_2 = \alpha \cdot k_{sec}$	[MPa/mm]

* Ω see next chapter

The parameter $\tau_{m,0}$ and $\tau_{f,0}$ represent the strength of the mechanical and frictional component (subscript m and f), respectively, for the case of no confining pressure, no damage and elastically behaved reinforcing bar element.

Up to the slip s_1 at which peak bond strength is reached (see Figure 4), all response curves are defined by Menegotto-Pinto (MP) equation /MENEGOTTO-PINTO, 1973/. The curve defines a curve connecting two line segments and it reads:

$$\tau(s) = \tilde{\tau} \cdot \tau_0 = \tilde{s} \cdot \left[b + (1-b) \cdot \left(\frac{1}{1+\tilde{s}^R} \right)^{\frac{1}{R}} \right] \cdot \tau_0 \qquad \textbf{(1)}$$

where b is the ratio between the target and initial tangents, $\tilde{\tau}$ and $\tilde{s}$ are normalized stress and displacement, respectively, and R defines the radius of the curvature. τ_0 and s_0 are the parameters to calculate the absolute stress and displacement from the normalized parameters.

$$b = \frac{k_2}{k_1} \tag{2}$$

$$k_2 = \alpha \cdot k_{secant} \quad , \quad \text{with} \quad 0 \le \alpha \le 1 \tag{3}$$

$$\tilde{s} = \frac{s}{s_0} \tag{4}$$

$$s_0 = s_1 \cdot \frac{(k_{secant} - k_2)}{k_1 - k_2} = s_1 \cdot k_{secant} \cdot \frac{(1-\alpha)}{k_1 - \alpha \cdot k_{secant}} \tag{5}$$

$$\tau_0 = s_0 \cdot k_1 \tag{6}$$

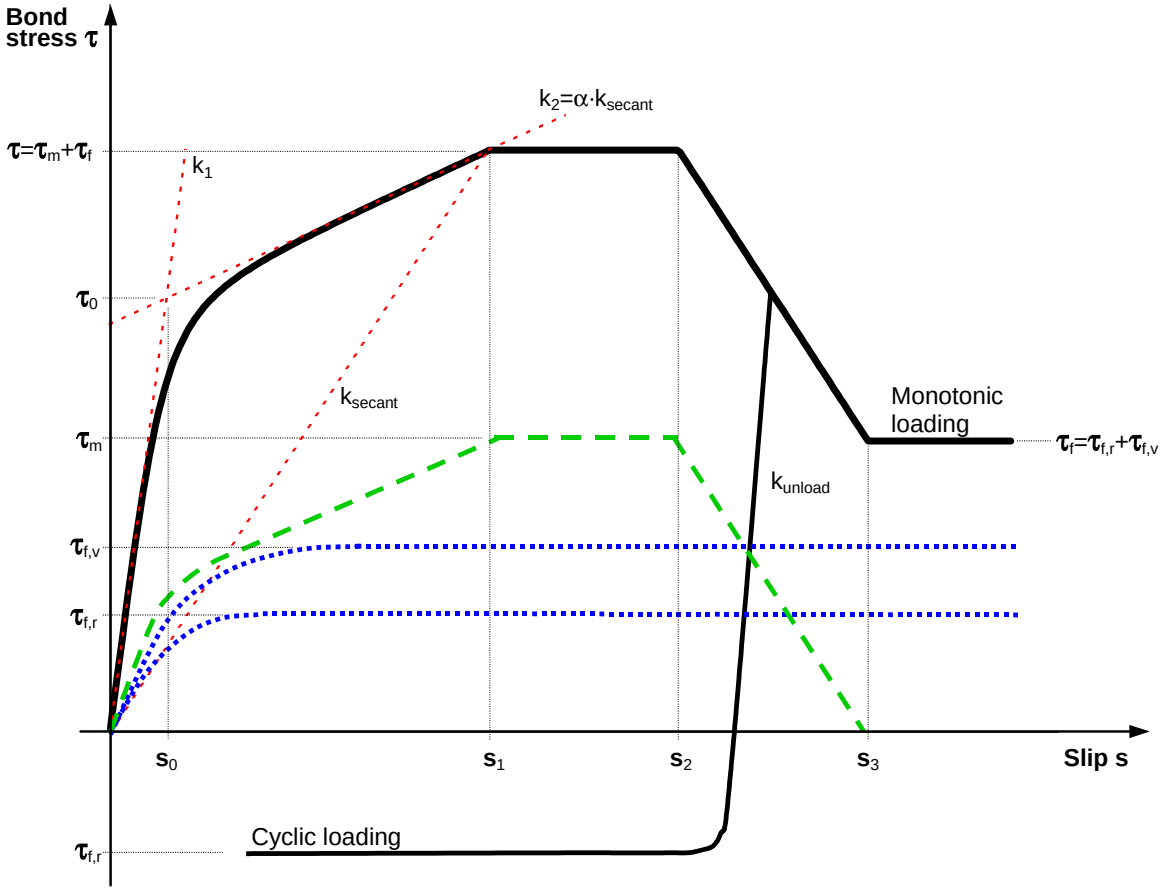

Figure 4: Bond stress-slip relation of the bond element model

Variation of bond strength in a 3D stress field

A factor Ω (see Table 1) accounts for the dependency of the bond stress on the stress-strain state of concrete and steel in the vicinity of the bond zone. As a result, the two dimensional bond stress versus slip relationship shown before is influenced by lateral expansion or extension in different ways and becomes a three dimensional model.

The parameter Ω is calculated as shown in equation (7). Three parameters are considered: Ω_S controls the influence of the yielding of steel reinforcement on the bond response and is set to Ω_S=1 for textile reinforcement; Ω_C accounts for the influence of the lateral stresses between reinforcement and concrete caused by the stress in concrete and the local strain of the bar element and its lateral expansion or extension; Ω_{cyc} controls the influence of the loading-unloading-reloading on the bond response.

$$\Omega = \Omega_S \cdot \Omega_C \cdot \Omega_{cyc} \tag{7}$$

As shown in equation (8) and Figure 5, the parameter Ω_C, which can theoretically vary between 0 and 2, accounts for two different effects. The first is the influence of the lateral strain of the stressed bar element. The parameter h_R is a constant that represents the surface roughness of the reinforcement bar. Compared to the ribbed reinforcement, h_R is close related to the height of the steel lugs. ε_s is the reinforcement strain, $d_s = 2r_s$ the bar diameter and μ_s is the Poisson's ratio of the used reinforcement element. The factor α_r controls the influence of the radial concrete stress and for the calculations is set to 1. The parameter α_f controls the influence of the roughness of the reinforcement h_R on the bond response. In the present study it was set to 2.

The parameter $\varepsilon_{p,0}$ is the strain due to prestressing of reinforcement. Consequently in the case of prestressing and non external loading the bond is increased only by the radial stress in concrete nearby the reinforcing bar.

$$\Omega_c = 1{,}0 + \tanh\left(\alpha_r \cdot \frac{\bar{\sigma}_R}{0{,}1 \cdot f_c} - \alpha_f \cdot \mu_s \cdot (\varepsilon_s - \varepsilon_{p,0}) \cdot \frac{1}{1 - \frac{r_s^2}{(r_s + h_R)^2}} \right) \tag{8}$$

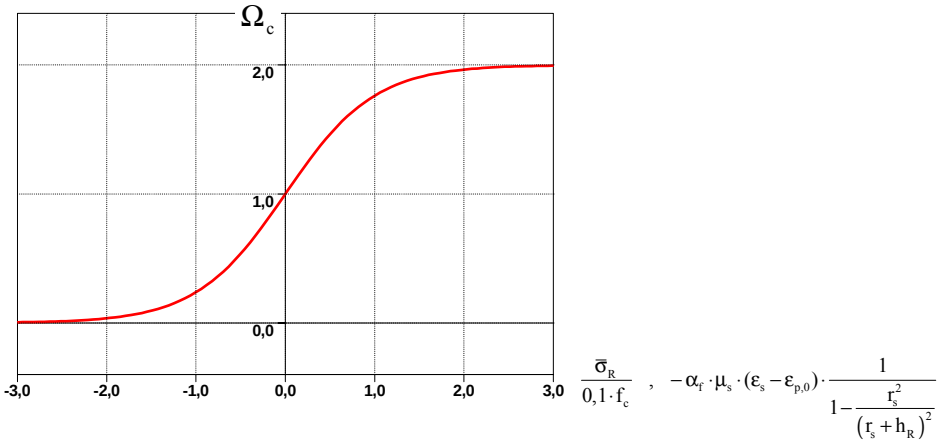

Figure 5: Definition of Ω_C as a function of lateral stress and strain

The influence of the radial stress in concrete in the vicinity of the reinforcing bar is accounted for by an average radial stress $\bar{\sigma}_r$ perpendicular to the bar direction. The parameter f_c is the uniaxial compressive strength of concrete. In the finite element analysis the average radial stress associated to the n-th bar element is calculated as:

$$\bar{\sigma}_r = \frac{1}{V_R}\sum_{i=1}^{N}\sigma_r^i \Delta V_i \quad \text{with} \quad V_R = \sum_{i=1}^{N}\Delta V_i \tag{9}$$

where ΔV_i denotes the volume which corresponds to the i-th integration point of the finite element and σ_r^i the stress perpendicular to the reinforcement. N is a total number of integration points that fall into a cylinder of a diameter D (see Figure 6). In the presented model D is assumed to be three times a bar diameter ($D \approx 3\, d_s$). In (9) V_R is the representative volume, i.e. the volume of the concrete cylinder of diameter D that is associated to the truss finite element which represents a reinforcing bar.

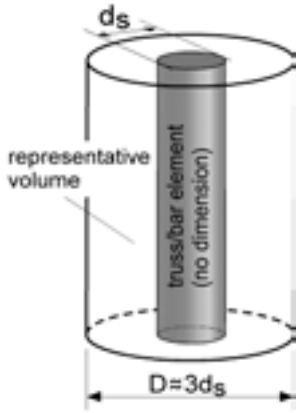

Figure 6: Representative volume

Experiments show that for cycling loading-unloading-reloading the bond strength significantly decreases with increase of number of loading cycles /ELIGEHAUSEN, 1983/, /BALAZS, 1991/. In the present model this effect is accounted for by the factor Ω_{cyc} that reads:

$$\Omega_{cyc} = \exp\left(-1.2 \cdot \left(\frac{\Lambda}{\Lambda_0}\right)^{1.1}\right) \tag{10}$$

where Λ is the accumulated shear energy dissipation and Λ_0 is a constant representing the area under the monotonic bond-slip curve of respective shear component. The above equation has been proposed by /ELIGEHAUSEN, 1983/ and it is based on a large number of cyclic test data of steel reinforced concrete.

Similar behavior seems also to be approximately valid for textile reinforced concrete, however, it is not clarified up to now.

NUMERICAL STUDIES

As shown in the last chapter the bond performance of the model is influenced by Ω_C which accounts for: (i) the influence of radial stress obtained from the surrounding concrete elements and (ii) the influence of reinforcement strain. To demonstrate the effects of these two different influences numerical studies have been carried out.

Two FE models (M_I and M_{II}) were employed to show the influence of the transverse stress field and the reinforcement strain on the bond properties. The FE mesh of these models is shown in Figure 7. It represents concrete specimen confined in direction x and y. The boundary conditions were slightly different. Model I (M_I) has some restrained nodes in the z-direction only at the bottom surface, where the load is applied to the bar element. In Model II (M_{II}) all the nodes over the specimen height were fixed in the z-direction. Consequently, the transverse stress field around the bar element is different. The bar element itself is placed in the middle of the specimen and is pulled in z direction at the point z = 20 mm (bottom surface).

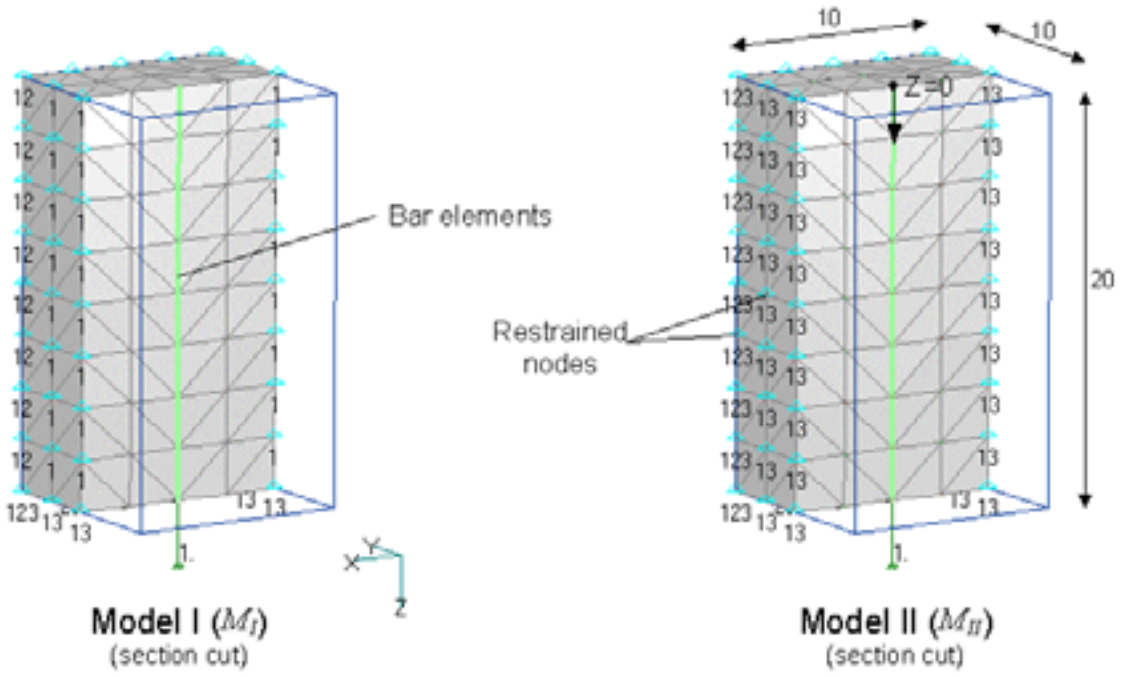

Figure 7: Finite element models with different boundary conditions

As shown in table 2, the main bond parameters were set to constant for all calculations. Note that these parameters were chosen only to qualitatively show the performance of the model and were not calibrated for the use in the practical

applications. Additionally, it has to be noted that the reinforcement is assumed to be linear elastic for all the calculations, i.e. $\Omega_S = 1$.

Table2: Summary of the used model parameters for the reinforcement

Description of the model parameter	Model parameter	
peak mechanical bond strength	$\tau_m = 9.0$	[MPa]
peak frictional bond strength	$\tau_f = 4.0$	[MPa]
secant to bond response curve for initial loading	$k_{sec} = 50.0$	[MPa/mm]
slip at which bond strength begins to decrease	$s_2^* = 0.03$	[mm]
slip at which mechanical bond resistance is lost	$s_3 = 0.50$	[mm]
tangent to the load-displacement curve upon unloading	$k_{unload} = 220.0$	[MPa/mm]
initial tangent to the bond-slip response	$k_1 = 220.0$	[MPa/mm]
tangent to the bond-slip curve at peak resistance	$k_2 = 22.0$	[MPa/mm]
radius of the curvature	$R = 8.0$	[-]
Poisson's ratio	$\mu_s = 0.5$	[-]
Young modulus	$E_s = 74000.0$	[MPa]
reinforcement area	$A_s = 0.93$	[mm²]
bar diameter	$2 \cdot r_s = 1.0$	[mm]
surface roughness	$h_R = 0.01$	[mm]

Moreover, to demonstrate the effect of prestressing, three different cases (a,b,c) were considered with:

$$\text{(a)} \quad \Omega_{C,a} = 1.0 \tag{11}$$

$$\text{(b)} \quad \Omega_{C,b} = 1.0 + \tanh\left(\frac{\bar{\sigma}_R}{0{,}1 \cdot f_c}\right) \tag{12}$$

$$\text{(c)} \quad \Omega_{C,c} = 1.0 + \tanh\left(\frac{\bar{\sigma}_R}{0{,}1 \cdot f_c} - \alpha_f \cdot \mu_s \cdot (\varepsilon_s - \varepsilon_{p,0}) \cdot \frac{1}{1 - \frac{r_s^2}{(r_s + h_R)^2}}\right) \tag{13}$$

Influence of the 3D stress field on the bond

In Figure 8 the results of the pull out stress versus slip are shown. In the case (a) the stress versus slip curve of both models looks almost the same for prestressed and non prestressed state, i.e. the concrete strain in z direction is negligible. Therefore it is shown only one curve. However, it can be seen that if

the reinforcement is prestressed maximum pullout stress increases slightly due to the more homogeneous bond stress distribution over the embedment length. For different cases at maximum load also see Figure 9. This effect can also be seen in all the calculation discussed later.

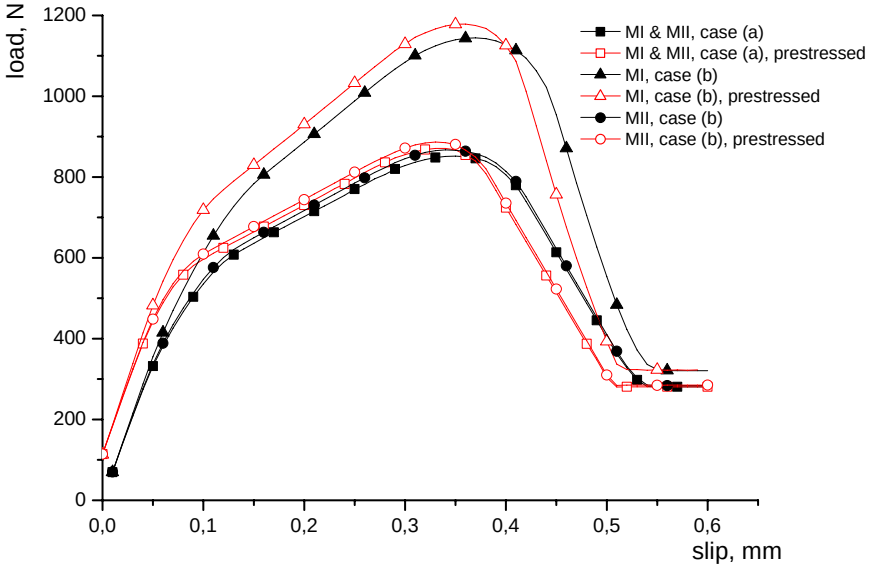

Figure 8: Calculated pull out load versus slip

If case (b) is considered and the influence of the radial stress of the concrete is taken into account, the change of bond response becomes obvious. The influence calculated in model M_{II} is almost insignificant whereas in model M_I maximum pull out stress increases over 30 percent caused by the deformation of the concrete elements. Additionally the bond stress is calculated as 1.5 times as high as for case (a) at z = 15mm which can be explained by the boundary conditions and the resulting stress field of concrete.

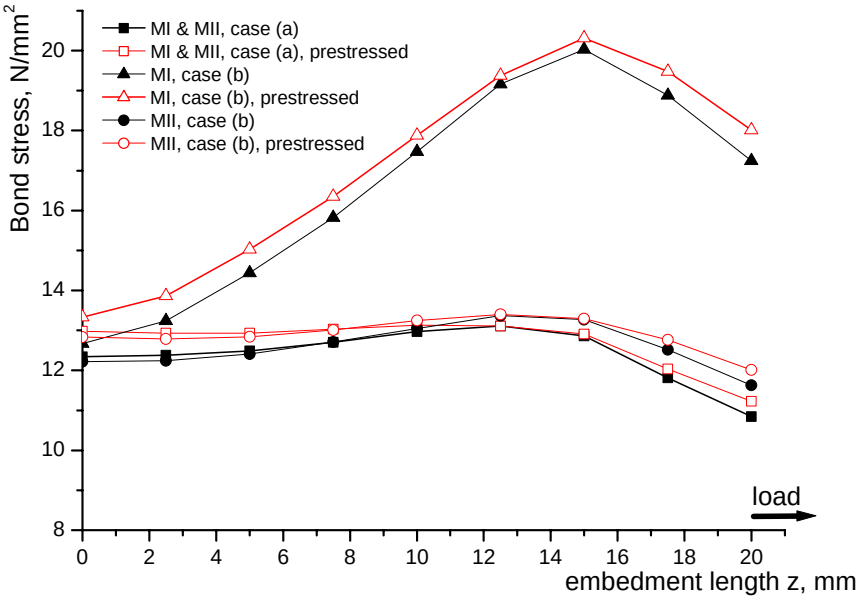

Figure 9: Comparison of calculated bond stress at maximum pull out load

Influence of the reinforcement strain on the bond performance

The results of the calculations of the pull out stress versus slip for case (c) are shown in Figure 10. For the model M_I the maximum load is just about 15 percent higher than for case (a) and lower than for case (b). Also the bond stress over the embedment depth is lower for case (c) compared to case (a), as shown in Figure 12.

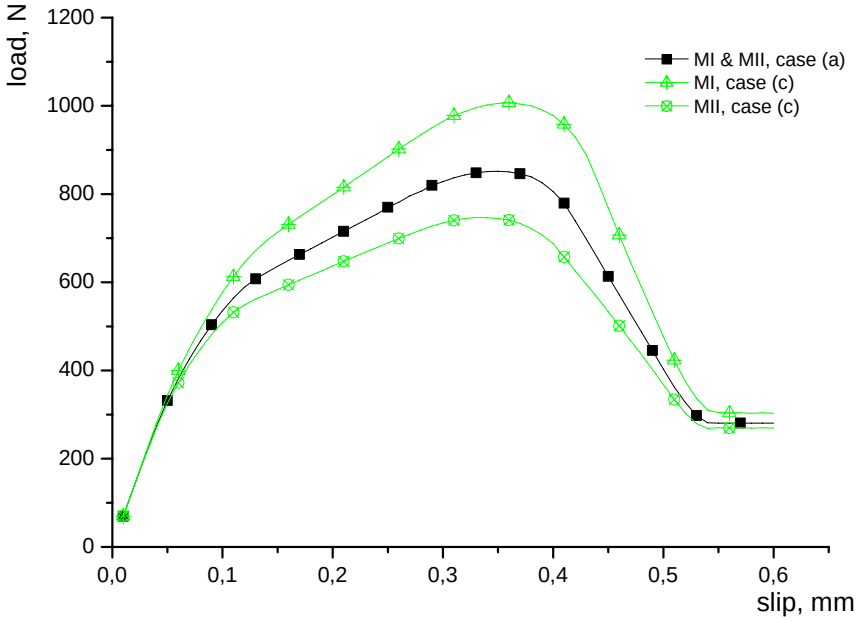

Figure 10: Calculated pull out load versus slip

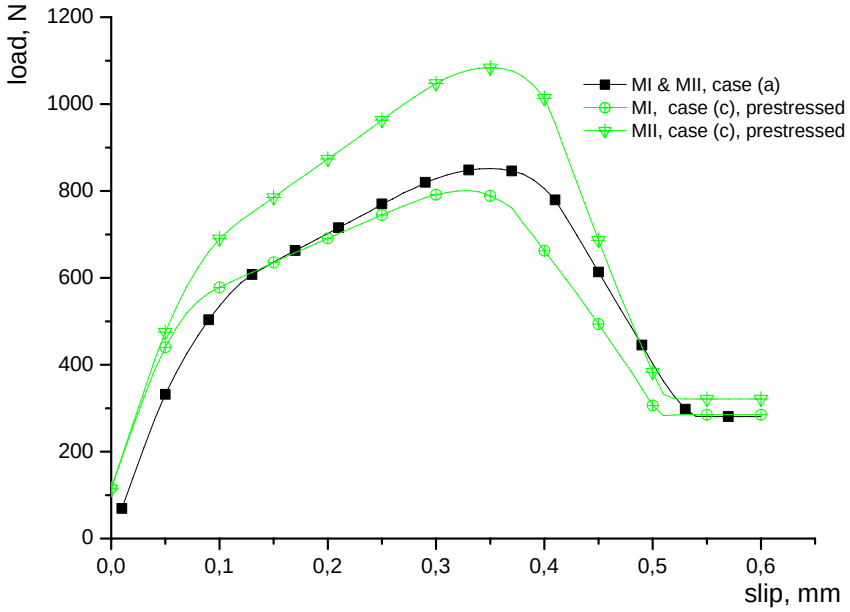

Figure 11: Calculated pull out load versus slip of prestressed specimen

In the calculated bond stress slip curves for prestressed reinforcements, shown in Figure 11, the influence of the steel strain on the bond performance is also obvious. Due to the prestressing of adhesive type, at initial state the reinforcement lateral strains are negative (compression). Consequently, the contraction of reinforcement is less than in the case of unprestressed reinforcement and therefore it does not result in such a large reduction of bond stresses. Figure 12 shows the influence of Ω_C on the bond stress for unprestressed and prestressed reinforcement.

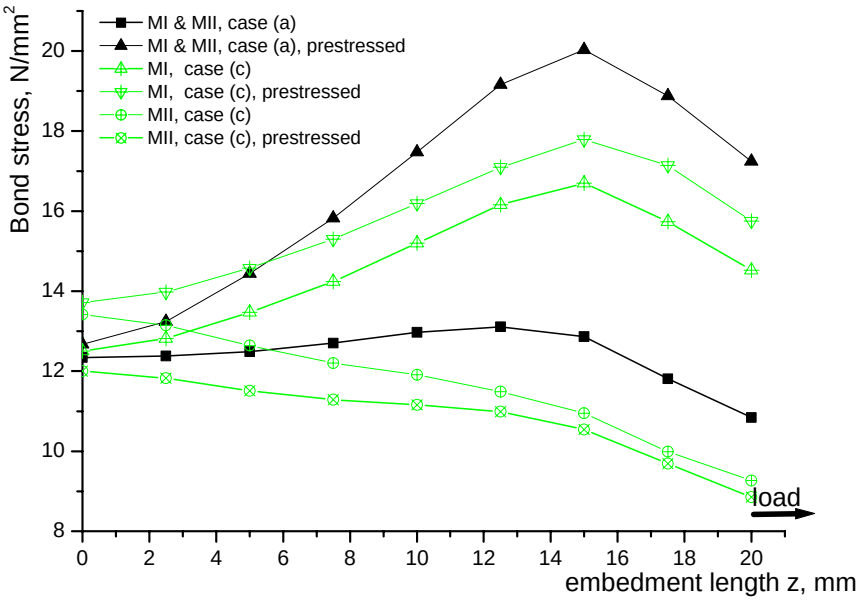

Figure 12: Comparison of calculated bond stress at maximum pull out load

Comparison of calculations and tests of textile reinforced elements in a bending test

In Figure 13 the result of a four-point bending test is compared with the results of the FE calculations. The span of the plate was 250 mm and the load was applied at the third points. The test specimen was a epoxy impregnated carbon textile reinforced concrete plate (300mm x 60mm x 10mm) with a fine grain concrete ($f_c \approx 80$MPa). The input parameters for the calculation of the bending test were calibrated at double sided pullout tests. For details see /KRÜGER, 2002/. For the calculation concrete is modelled by the microplane model. The agreement between simulation and experimental results is good. However, compared to the test results, the numerical results show in the post peak region more ductile behaviour.

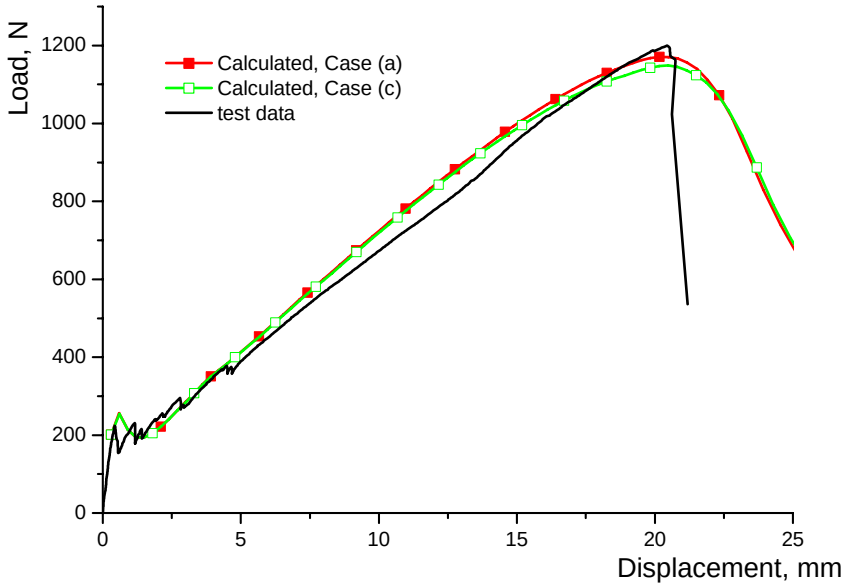

Figure 13: Load-deflection curve for a carbon reinforced element under monotonic loading

As can be seen from Figure 14, the strain in x direction (dark zones indicate cracks) show a good agreement with the crack distribution observed in the experiment. It has to be noted that the crack distribution in the tested specimen is greatly influenced by the transverse textile reinforcement, which leads to less cracks but a higher crack width.

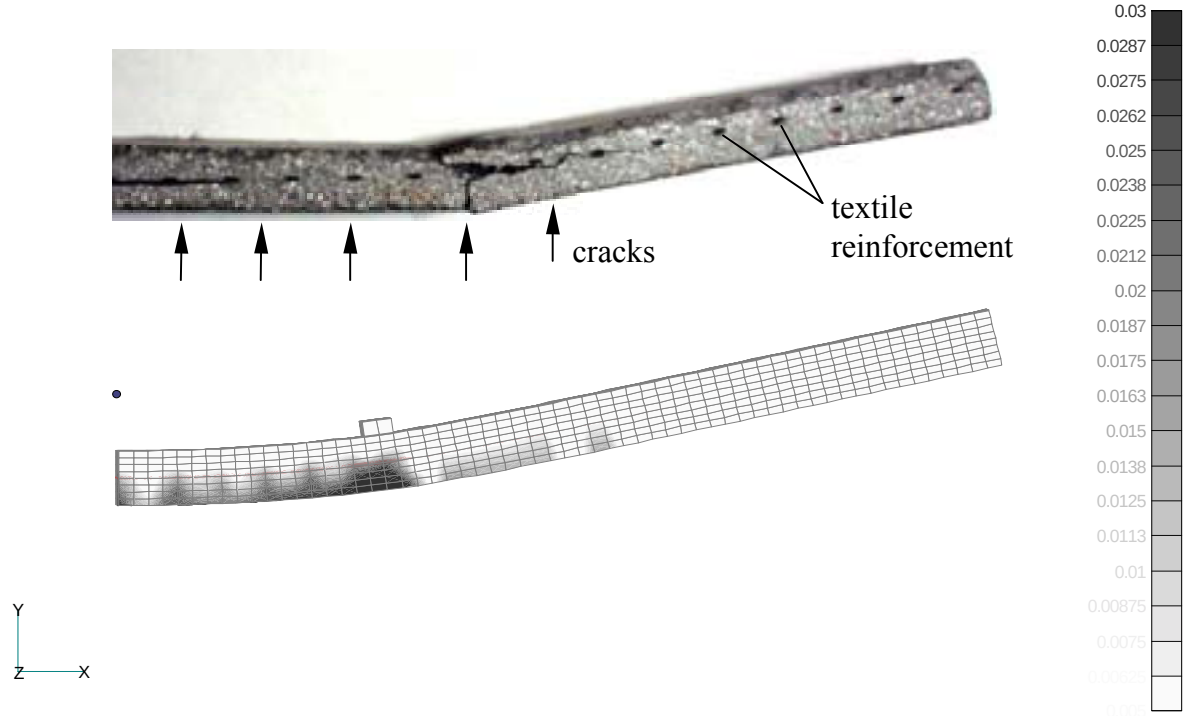

Figure 14: Comparison of principle strains of calculated model in x direction at maximum load and crack distribution of tested specimen.

In Figure 15 the strains of the concrete elements in y direction (horizontal cracks) are shown and compared with specimen. The dark zones represents cracked concrete. In the experiment almost the same crack distribution and the same failure mode was observed.

Figure 15: Comparison of tested specimen after test and principle strains of concrete elements in y direction at maximum load.

CONCLUSIONS

A new discrete bond model that is based on a bond stress-slip relationship has recently been implemented into a 3D finite element code. The bond model accounts for the influence of elastic and plastic reinforcement strains, the influence of the radial stress of the surrounding concrete as well as for the influence of the cyclic load history on the bond response.

As shown in the numerical examples, the transverse stress field and the reinforcement strain may have significant influence on the local bond stress. If a reinforcement with a rough surface is used the local bond stress is mainly influenced by the radial stress of the surrounding concrete. However, the influence of the reinforcement strain increases as smoother the reinforcement surface is.

The parameter Ω_C influences the local failure of concrete close to the bar nearby a crack where relatively high stresses in reinforcement are present. The bond strength is reduced and therefore crack width and the distribution of cracks is affected. It is well known that also yielding of steel reinforcement enlarge this effect which is accounted for by Ω_S in the bond model.

The benefit of the presented bond model becomes obvious if one consider different types of reinforcements, e.g. different diameter, surface structures or steel lugs and stress strain properties. It is assumed that the general parameters of the bond stress slip-relation shown in Figure 1 mainly depend on the concrete parameters and can be set to constant for a group of reinforcement elements of the same type. This can be for example a set of steel bars of different diameter or textile reinforcement type with different Young's modulus but almost the same surface roughness.

Nevertheless the discussed model have to be calibrated based on a series of different experimental tests in order to find out the real influence of transverse stresses and strains on the bond response and thus on the structural response as well.

REFERENCES

Balazs, G.L. (1991): *Fatigue of bond*. ACI Materials Journal, 88 (6), 620-629, 1991.

Brameshuber, W.; Banholzer, B.; Brümmer, G. (2000): *Ansatz für eine vereinfachte Auswertung von Faser-Ausziehversuchen*. Beton- und Stahlbetonbau, No. 95, Heft 12, pp. 702-706, 2000.

CEB Bulletin 230 (1996*): RC elements under cyclic loading*. State of the art report, Ed. By T. Telford, Thomas Telford Service Ltd, London, 1996.

Curbach, M.; Zastrau, B. (1999): *Textilbewehrter Beton – Aspekte aus Theorie und Praxis*. Baustatik-Baupraxis 7, Meskouris (Ed.), Balkema, Rotterdam, 1999.

Eligehausen, R.; Popov, E.P.; and Bertero, V.V. (1983): *Local Bond Stress-Slip Relationships of Deformed Bars under Generalized Excitations.* Report UCB/EERC-83/23. Berkeley: EERC, University of California, 1983.

Krüger, M. (2001a): *Prestressed Textile Reinforced Cement Composites.* IWB-Mitteilungen, Jahresbericht 2000/2001, University of Stuttgart, Institute of Construction Materials (IWB), 2001.

Krüger, M.; Reinhardt, H.-W.; Fichtlscherer, M. (2001b): *Bond behaviour of textile reinforcement in reinforced and prestressed concrete*. In: Otto-Graf-Journal. Vol. 12 2001, pp. 33-50.

Krüger, M.; Reinhardt, H.-W. (2001c): *Prestressed textile reinforced cement composites*. Proc. „11. Internationale Techtextil-Symposium für technische Textilien, Vliesstoffe und textilarmierte Werkstoffe", No. 338, Frankfurt, Apr. 2001.

Krüger, M.; Xu, S.; Reinhardt, H.-W.; Ožbolt, J. (2002): *Experimental and numerical studies on bond properties between high performance fine grain concrete and carbon textile using pull out tests*. In: Beiträge aus der Befestigungstechnik und dem Stahlbetonbau (Festschrift zum 60. Geburtstag von Prof. Dr.-Ing. R. Eligehausen), pp. 151-164, Stuttgart, 2002.

Lowes, L. N.; Moehle, J.P.; Govindjee, S. (2002): *A concrete-steel bond model for use in finite element modelling of reinforced concrete structures*. In print, 2002.

Malvar, L.J. (1992): *Bond reinforcement under controlled confinement*. ACI Materials Journal 89 (6), 711-721, 1992.

Menegotto, M.; Pinto, P. (1973): *Method of analysis of cyclically loaded reinforced concrete plane frames including changes in geometry and nonelastic behaviour of elements under combined normal geometry and nonelastic behaviour of elements under combined normal force and bending*. Proceedings of the IABSE Symposium on the resistance and ultimate deformability of structures acted on by well-defined repeated loads, Lisbon, 1973.

Nammur, G.; Naaman, A. (1989): *Bond Stress Model for Fiber Reinforced Concrete Based on Bond Stress-Slip Relationship*. ACI Materials Journal, No. 86, pp. 45-55, Jan./Febr. 1989.

Ohno, S.; Hannant, D.J. (1994): *Modelling the stress-strain Response of Continuous Fibre Reinforced Cement Composites*. ACI Materials Journal, No. 91, pp. 306-312, Mar. 1994.

Ožbolt, J.; Li Y.; Kožar, I. (2001): *Microplane model for concrete with relaxed kinematic constraint*. Int. J. of Solids and Structures, 38, 2683-2711, 2001.

Ožbolt, J.; Lettow, S.; Kožar, I. (2002): *Discrete bond element for 3D FE analysis of reinforced concrete structures*. In: Beiträge aus der Befestigungstechnik und dem Stahlbetonbau (Festschrift zum 60. Geburtstag von Prof. Dr.-Ing. R. Eligehausen), pp. 239-258, Stuttgart, 2002.

Reinhardt, H.-W.; Krüger, M. (2001): *Vorgespannte dünne Platten aus Textilbeton*. Proc. „Textilbeton – 1. Fachkolloquium der Sonderforschungsbereiche 528 und 532“, edited by J. Hegger, pp. 165-174, Aachen, 2001.

Yankelevsky, D.Z.; Reinhardt, H.-W. (1987): *Response of plain concrete to cyclic tension*. ACI Materials Journal 84 (5), 365-373 1987.